Computational Modelling of Cerebellar Magnetic Stimulation: The Effect of Washout

Alberto Antonietti[1,2(✉)], Claudia Casellato[2], Egidio D'Angelo[2,3], and Alessandra Pedrocchi[1]

[1] Politecnico di Milano, Piazza Leonardo da Vinci 32, 20133 Milan, Italy
alberto.antonietti@polimi.it
[2] University of Pavia, Via Forlanini 6, 27100 Pavia, Italy
[3] IRCCS Mondino Foundation, Via Mondino 2, 27100 Pavia, Italy

Abstract. Nowadays, clinicians have multiple tools that they can use to stimulate the brain, by means of electric or magnetic fields that can interfere with the bio-electrical behaviour of neurons. However, it is still unclear which are the neural mechanisms that are involved and how the external stimulation changes the neural responses at network-level. In this paper, we have exploited the simulations carried out using a spiking neural network model, which reconstructed the cerebellar system, to shed light on the underlying mechanisms of cerebellar Transcranial Magnetic Stimulation affecting specific task behaviour. Namely, two computational studies have been merged and compared. The two studies employed a very similar experimental protocol: a first session of Pavlovian associative conditioning, the administration of the TMS (effective or sham), a washout period, and a second session of Pavlovian associative conditioning. In one study, the washout period between the two sessions was long (1 week), while the other study foresaw a very short washout (15 min). Computational models suggested a mechanistic explanation for the TMS effect on the cerebellum. In this work, we have found that the duration of the washout strongly changes the modification of plasticity mechanisms in the cerebellar network, then reflected in the learning behaviour.

Keywords: Brain simulation · Cerebellum · Spiking Neural Networks · TMS · Neurostimulation

1 Cerebellar Transcranial Magnetic Stimulation

Transcranial magnetic stimulation (TMS) is a noninvasive technique that can be used to study, diagnose, or treat neural pathologies. A coil induces a magnetic

This project has been developed within the CerebNEST HBP Partnering Project and has received funding from the European Unions Horizon 2020 Framework Programme for Research and Innovation under Grant Agreement No. 785907 (Human Brain Project SGA2).

K. Amunts et al. (Eds.): BrainComp 2019, LNCS 12339, pp. 35–46, 2021.
https://doi.org/10.1007/978-3-030-82427-3_3

field that generates an electric field in the brain tissue. The electric field directly interferes with nervous system functions by changing the electrical behaviour of neurons.

Among the different protocols that are available for TMS, continuous theta-burst stimulation is usually delivered to influence long-term plasticity changes. The stimulation protocol can consist of pulse bursts 50 Hz repeated every 200 ms, given in a continuous train lasting tens of seconds. The stimulation intensity is calibrated using the active motor threshold, defined as the lowest intensity stably evoking motor-evoked potentials. Common values for the stimulation amplitudes for theta-burst TMS range between 0.5 and 0.7 kV, generating a peak magnetic field of ∼1 T reaching a depth of 20–30 mm from the scalp surface [13].

Cerebellar TMS foresees the administration of the stimulation over one cerebellar hemisphere or the cerebellar vermis, and it can be used during cerebellar-driven protocols to interfere with the learning processes at neural level. It has been shown that cerebellar TMS stimulation influences the learning processes, but the underlying mechanisms are still unconfirmed [7,10,12,16].

In order to better understand the effects of cerebellar TMS, both experimental and computational approaches have been used in the last years.

2 Experimental Protocols

Monaco and colleagues [13,14] have employed TMS stimulation on human participants between two sessions of eyeblink conditioning protocol (EBC), a temporal associative task in which the subject learns, thanks to cerebellar plasticity, the precise timing associations between two stimuli. In EBC, the participant learns the association between a neutral conditioned stimulus (e.g., a sound) and a following unconditioned stimulus, eliciting an eyeblink (e.g., an electric shock near the eye). Initially, subjects respond with a reflexive eyelid closure, following the unconditioned stimulus. Along with learning of this association, participants start to express a Conditioned Response (CR), anticipating the unconditioned stimulus.

The two EBC studies [13,14] have common features, such as the presence of two consecutive sessions of EBC ($session_1$ and $session_2$), each one composed of 6 blocks of acquisition, where two stimuli were provided to the subject, and one block of extinction, where only one stimulus was provided to the subject. In the acquisition phase, the subject learns the timing association between the two stimuli, thus exhibiting an increasing percentage of correct CRs. In the extinction phase, the subject unlearns the association between the two stimuli, since the second one no more follows the first one. In both studies, an effective or a sham cerebellar TMS stimulation was administered at the end of the first session. The studies aimed at investigating the behavioural differences between the TMS and the control (sham) groups in the second session.

There are some minor discrepancies between the two experimental protocols (see Table 1), but the most important one is the washout period between the first and the second session of EBC: a long one (i.e., 1 week) in Monaco et al. 2014 [13], and a short one (i.e., 15 min) in Monaco et al. 2018 [14].

Table 1. Details of the two EBC experimental protocols

Property	Monaco et al. 2014	Monaco et al. 2018
Number of subjects for each group	11	12
Number of groups	2	3
Stimulated hemisphere	Right	Right or left
Number of trials per block	10	11
Inter-stimulus interval	600 ms	400 ms
Washout period	1 week	15 min

In both experimental datasets, changes in the learning and unlearning trajectories of CRs between the TMS and the control groups were observed. Namely, with a long washout, the TMS group showed impairment in the extinction phase of $session_2$ (from block 6 to block 7), where the unlearning resulted in being slowed down (Fig. 1.A). With a short washout, the TMS groups (right or left stimulated hemisphere) showed a less effective relearning phase at the beginning of acquisition (block 1 of $session_2$) and, again, a slowed down unlearning during the extinction phase (Fig. 1.B).

Overall, the findings from both experimental studies suggested that TMS can impair memory consolidation processes in the cerebellum, possibly by interfering with memory transfer from the cerebellar cortex to deeper structures. However, due to the noninvasive nature of TMS investigation, it was possible to only speculate about the putative mechanisms underlying the behavioural differences. To have a greater insight about the neural processes involved by the TMS, a computational approach was used in two previous works [1,3].

3 Computational Modelling

Historically, computational models of the brain have been widely used to acquire new knowledge that cannot be obtained from physiological studies and abstract theories. These models proved to be a powerful tool that can support the other approaches in tackling the complex problem of understanding how the brain works. Spiking Neural Networks (SNNs) have been used to mimic the neural organization, employing single units (i.e., the neurons) organized and connected similarly to the relative biological structures [4,9].

Recently, a detailed spiking neural network model of the cerebellar microcircuit proved able to reproduce multiple cerebellar-driven tasks [5], among which the EBC paradigm [2]. Having been validated, the SNN model was challenged to fit the two experimental datasets recorded by Monaco and colleagues from human subjects [13,14], with a long [1] or a short washout [3]. In both studies, the SNN model was able to capture the specific alterations in the second EBC session caused by TMS interference. Indeed, TMS affected motor response evolution along task repetitions, and we inferred the underpinning plasticity changes over the whole network.

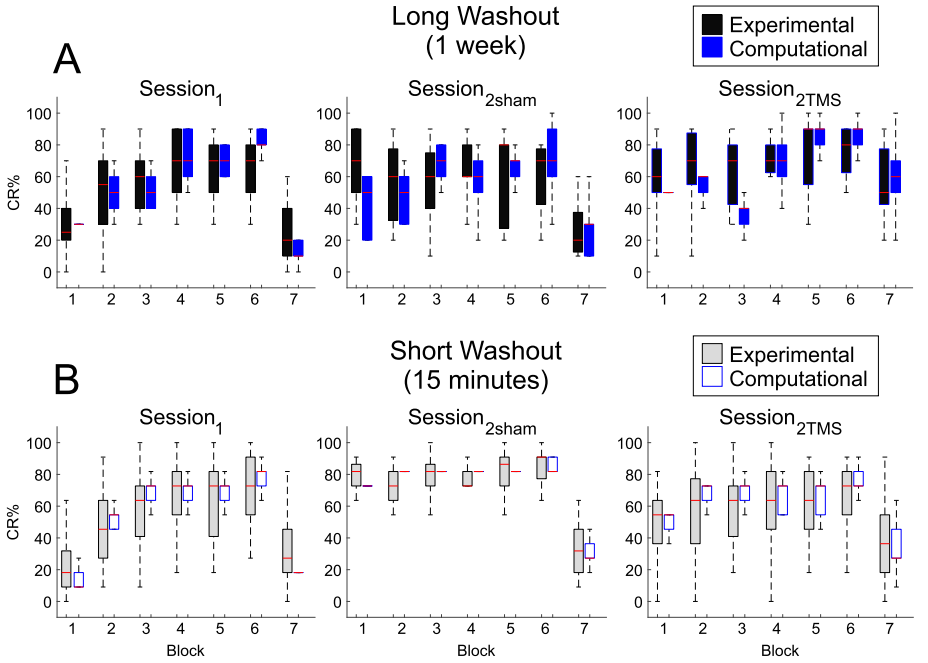

Fig. 1. CR percentages in experimental and modelling studies. A) Box-plots of CR percentages along the seven blocks of the EBC protocol with a long washout (1 week) between $session_1$ and $session_2$. Left panel: $session_1$, Central panel: $session_2$ with sham TMS, Right panel: $session_2$ with effective TMS. Boxes represent the upper and lower quartiles, the whiskers identify the range, and the red lines represent median values. Black boxes represent experimental data from [13] and blue boxes represent modelling data from [1] B) Box-plots of CR percentages along the seven blocks of the EBC protocol with a short washout (15 min) between $session_1$ and $session_2$. Grey boxes represent experimental data from [14], and white boxes represent modelling data from [3]. (Color figure online)

The SNN cerebellar microcircuit was populated with leaky Integrate&Fire neurons, distinguishing between different neural groups. Mossy Fibers (MFs), the input neurons of the system, encode the first (conditioned) stimulus. In fact, it has been shown that these neurons encode the state of the system (e.g., the presence of a certain sound). Granular Cells (GrCs) represent in a sparse way the input from the MFs. Inferior Olive neurons (IOs), the other input to the system, encode the second (unconditioned) stimulus, since this neural population is active in presence of pain. Purkinje Cells (PCs) integrate the sparse information coming from the GrCs through the Parallel Fibers (PFs), while Deep Cerebellar Nuclei (DCNs), the only output of the cerebellar microcomplex, activate the motor response (i.e., the anticipatory CR). While the network structure and connectivity are the same in the two computational studies (Fig. 2), the number of neurons for each population is different, as reported in Table 2, since

the SNN used in Antonietti et al. 2018 is three-times larger than the one used in Antonietti et al. 2016. Both studies used EDLUT simulator environment to perform the neural simulations [17].

The connectivity between the different neural populations follows the same rules. MFs send projections to the GrCs, each GrC receives input from 4 MFs; IOs send one-to-one teaching connections to PCs; DCNs receive both excitatory

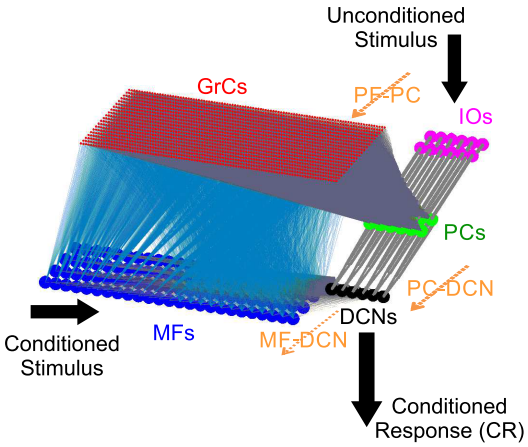

Fig. 2. Spiking Neural Network model used to simulate the cerebellar circuit. Both computational studies [1,3] used the same network architecture, but with a different number of neurons for each neural population (see Table 2). Circles represent neurons and lines represent synaptic connections. Plasticity sites are marked by orange labels. The first (conditioned) stimulus is encoded by MFs, while the second (unconditioned) is encoded by IOs. The activity of DCNs is the network output and generates CRs. (Color figure online)

Table 2. Number of neurons and synapses of the SNNs cerebellar models

Neural population	Antonietti et al. 2016	Antonietti et al. 2018
MFs	100	300
GrCs	2000	6000
IOs	12	36
PCs	12	36
DCNs	6	18
Synaptic connection		
MF-GrC (static)	8000	24000
PF-PC (plastic)	19164	172806
IO-PC (static)	12	36
MF-DCN (plastic)	600	5400
PC-DCN (plastic)	12	36

inputs directly from MFs and inhibitory synapses from PCs. The SNN models has three plasticity sites, at cortical level (PF-PC) and at nuclear level, between MF-DCN and PC-DCN, all based on different kinds of Spike-Timing Dependent Plasticity (STDP) [6,11]. PF-PC plasticity is modulated by IO activity, MF-DCN by PC activity, while PC-DCN is a standard unsupervised STDP learning, depending only on the difference between the pre- and post-synaptic firing times [8,15,18]. Each learning rule encompasses two different plasticity mechanisms: Long Term Depression (LTD), decreasing the synapse strength, and Long Term Potentiation (LTP), strengthening the connection. Therefore, each plasticity site can be characterized by two constants that regulate the amount of synaptic change. These constants cannot be directly computed from physiological data; as a result, we have treated those as free parameters of the SNN model, to be optimized according to the desired behaviour. The two computational studies employed evolutionary algorithms to identify the best six parameters (PF-PC LTP, PF-PC LTD, MF-DCN LTP, MF-DCN LTD, PC-DCN LTP, and PC-DCN LTD) in each experimental condition ($session_1$, $session_{2sham}$, and $session_{2TMS}$).

Employing realistic SNN models, Antonietti and colleagues have shown how closed-loop simulations can be successfully used to fit real experimental datasets. Thus, the changes in the model parameters in the different sessions of the protocol unveil how microcircuit mechanisms let implicitly emerge healthy and altered behavioural functions. In this work, we have analyzed the data generated by experimental and computational studies, in order to clarify the role of the washout period, the main difference between the two datasets.

4 Comparative Analysis

The elements analyzed in the present study are the learning and unlearning trajectories (i.e., the variation in CR percentage between blocks) and the values of LTP and LTD parameters at the three plasticity sites that yielded to different behaviours in the simulations.

The two computational studies have already demonstrated that the behavioural response generated by the model in each block was a good representation of the experimental recordings. Figure 1 shows that the CRs generated by the model (blue boxes in Panel A, white boxes in Panel B) were comparable with the experimental results (black boxes in Panel A, grey boxes in Panel B). The degree of variability of the experimental data was higher than the computational studies, but a certain degree of variability was maintained. The variability in the results generated by SNN models was due to the fact that multiple combinations of LTP and LTD parameters have been considered. In fact, the evolutionary algorithm identified a family of optimal parameter combinations, leading to similar performances.

For the short washout protocol, two distinct TMS groups were identified, one receiving a stimulation of the left cerebellar hemisphere, the other one receiving the stimulation on the right hemisphere. Since there were no significant differences between the CRs recorded from the two groups, in the present study, the

results of both groups have been merged in a single TMS group, then compared to the sham group. In this way, we can make a direct comparison between the two studies, considering only two groups: sham vs TMS.

We focused our analysis on the two salient phases that were changed in $session_2$ for the TMS group with respect to the sham group. Namely, the fast acquisition (from zero to block 1, Fig. 3.A) and the extinction (from block 6 to block 7, Fig. 3.B). After a prolonged washout, the percentage of CRs acquired in the first block did not differ between the sham and the TMS groups. On the other hand, TMS slowed down the fast learning phase when a short washout interleaved the two EBC sessions (73% sham, 54.5% TMS, Fig. 3.A).

Conversely, the TMS administration interfered with the extinction phase after both long and short washouts. In fact, with a long washout the TMS group decreased the percentage of CRs of only −30% [−40 −10], while the sham group unlearnt faster −50% [−60 −40]. The same behaviour was observed with a short washout, where the extinction rate was −36% [−55 −27] in TMS group and −55% [−64 −45] in the sham group.

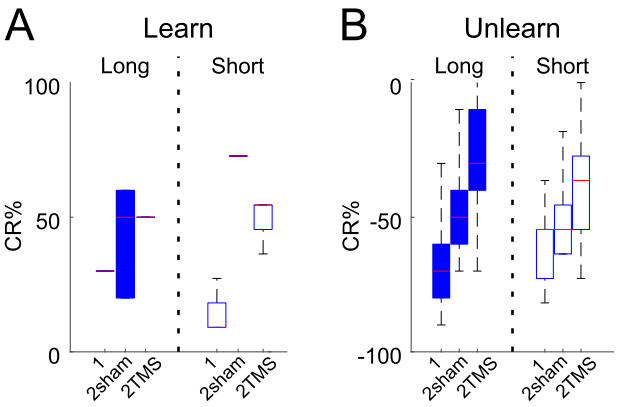

Fig. 3. Comparison of learning and unlearning rates in $session_1$, $session_{2sham}$, and $session_{2TMS}$. A) Fast learning rates, i.e., increase in CRs in the first acquisition block with long (left) or short (right) washouts. B) Unlearn rates, i.e. decrease in CRs from the last block of extinction (block 6) to the extinction (block 7). Boxes represent the upper and lower quartiles, the whiskers identify the range, and the red lines represent median values. Blue boxes represent modelling data from [1] and white boxes represent modelling data from [3]. (Color figure online)

Summarizing, the TMS affected both the fast acquisition and the extinction only with a short washout, while it impacted only the extinction phase with a long washout. We have then analyzed the LTP and LTD parameters of the SNN distributed plasticity that generated this different behaviour.

Figure 4 illustrates the overall variations of LTP and LTD parameters for the cortical plasticity (PF-PC, Panel A) and the nuclear plasticities (MF-DCN,

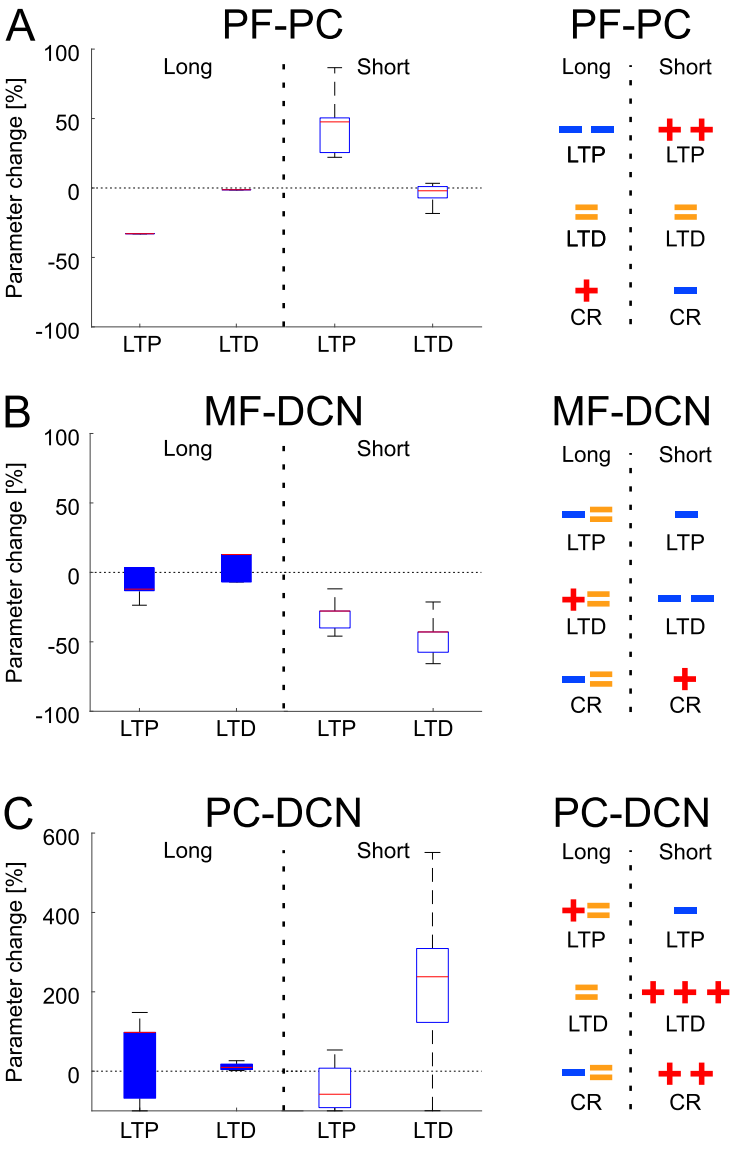

Fig. 4. Changes for LTP and LTD Parameter at the Three Different Plasticity Sites: A) PF-PC, B) MF-DCN, and C) PC-DCN. The left column represents box-plots of the parameter change in $session_2$ for the TMS group with respect to the parameter values for the sham group. Boxes represent the upper and lower quartiles, the whiskers identify the range, and the red lines represent median values. Blue boxes represent modelling data from [1] and white boxes represent modelling data from [3]. The right column presents a synthesis of the parameter changes (LTP and LTD) and the overall effect on the CR generation. Plus/minus symbols indicate qualitatively the amount of increase/decrease of the parameter in the TMS group or an increase/decrease in CR percentage generation. Equal symbols indicate negligible changes. (Color figure online)

Panel B, and PC-DCN, Panel C). The left column reports the percentage variation of the LTP and LTD parameters in the TMS group with respect to the sham group. An increased LTP parameter implicates a stronger potentiation of the synapses, while an increased LTD parameter entails a stronger weakening. The right column summarizes the combined effect of LTP and LTD changes and their effect on the CR generation process, that can be favoured or hindered.

Considering the PF-PC plasticity, it is possible to observe that while the LTD constant was not influenced by the TMS stimulation, the LTP parameter was decreased with a long washout and increased with a short one. This cause an increased and a decreased generation of CRs in the long and short washout case, respectively.

Considering the nuclear plasticities, the changes were limited for both LTP and LTD parameters in the long washout case. On the other hand, the changes were evident for the short washout case, where the variations of LTP and LTD parameters moved in favour of a generation of CRs. In fact, the LTD of the excitatory MF-DCN synapses was decreased, while the LTD of the inhibitory PC-DCN synapses was strongly increased. As a result, more excitatory inputs from the MFs and a weaker inhibition from the PCs increased the firing rate of DCN, thus generating more CRs.

5 Discussion and Conclusions

The analysis of LTP and LTD parameters showed that changes in behaviour with short and long washout are due to different rate in the rules driving synaptic modifications.

In particular, it can be observed that the administration of TMS followed by a prolonged washout caused a significant modification of the cortical plasticity only, with minor involvement of nuclear plasticities. Besides, the decrease of the PF-PC LTP parameter was in favour of a generation of CRs, therefore the fast acquisition in $session_{2TMS}$ was not impaired since the SNN expressed a high number of CRs, but this change impacted the extinction phase, where suppression of CRs was required.

In the case of a short washout, the parameters changed in a completely different way. First of all, it has been observed an involvement of both the cortical and the nuclear sites. While the cortical plasticity expressed a higher value of LTP, thus hindering CRs generation, the LTP and LTD constants of nuclear plasticities moved toward values that promoted CRs. As a matter of fact, the cortical and the nuclear mechanisms worked in opposite directions. This is the reason why, in the short washout case, both the learning and unlearning phases were impaired. The learning phase was slowed down by a weaker PF-PC response, while the reduced extinction was due to a higher DCN activity caused by the nuclear plasticities.

We can, therefore, conclude that the duration of the washout after the TMS administration is a crucial variable that can change the reorganization of plasticity and neural dynamics in the cerebellum. Since the TMS induces an electrical field in the most superficial areas of the tissue, the cortical plasticity is

the one primarily involved, as reflected by major changes concerning its LTP mechanisms (increasing or decreasing the potentiation effectiveness). However, if sufficient recovery time is granted, the TMS effect is limited to the cerebellar cortex and does not interfere with deeper systems (i.e., nuclear plasticities) and memory transfer. Viceversa, if the inter-session pause after TMS perturbation is shortened, the cortical impairment in the acquisition phase triggers a compensatory effect of the nuclear plasticities, that try to favour CRs generation, but on a longer time-scale. Then, the nuclear compensation becomes an obstacle during the extinction phase.

It is important to highlight that the effect of TMS is more evident for the short washout, both in the experimental and computational studies. In fact, $session_{2sham}$ and $session_{2TMS}$ experimental data for the long washout protocol show high variability during the acquisition blocks. At the same time, the computational model fit those blocks with less fidelity. The second EBC session after a long washout suffers from the interference of the neural activity and synaptic changes that naturally happen during one week of participants' life, where external stimuli and internal processes can disrupt or modify cerebellar memory formation and consolidation.

This work carried out a retrospective analysis and a comparison of TMS-perturbed EBC paradigms that present some differences both from the experimental protocol (see Sect. 2, Table 1) and the related computational studies (see Sect. 3, Table 2). However, we believe that this comparative analysis provides a summary of the mechanistic explanations that can be derived from the interpretation of the SNN model parameters, highlighting the effects of the washout period in studies that foresee the administration of (cerebellar) TMS on human participants.

Data Availability. Datasets and Codes to reproduce the findings and figures reported in this paper is publicly available at Harvard Dataverse (DOI: 10.7910/DVN/9HPEV4).

References

1. Antonietti, A., Casellato, C., D'Angelo, E., Pedrocchi, A.: Model-driven analysis of eyeblink classical conditioning reveals the underlying structure of cerebellar plasticity and neuronal activity. IEEE Trans. Neural Netw. Learn. Syst. **28**, 2748–2762 (2016). https://doi.org/10.1109/TNNLS.2016.2598190
2. Antonietti, A., et al.: Spiking neural network with distributed plasticity reproduces cerebellar learning in eye blink conditioning paradigms. IEEE Trans. Biomed. Eng. **63**(1), 210–219 (2016). https://doi.org/10.1109/TBME.2015.2485301
3. Antonietti, A., Monaco, J., D'Angelo, E., Pedrocchi, A., Casellato, C.: Dynamic redistribution of plasticity in a cerebellar spiking neural network reproducing an associative learning task perturbed by TMS. Int. J. Neural Syst. **28**(09), 1850020 (2018). https://doi.org/10.1142/S012906571850020X
4. Brette, R., et al.: Simulation of networks of spiking neurons: a review of tools and strategies. J. Comput. Neurosci. **23**(3), 349–398 (2007). https://doi.org/10.1007/s10827-007-0038-6

5. Casellato, C., et al.: Adaptive robotic control driven by a versatile spiking cerebellar network. PLoS ONE **9**(11), e112265 (2014). https://doi.org/10.1371/journal.pone.0112265
6. D'Angelo, E., et al.: Modeling the cerebellar microcircuit: new strategies for a long-standing issue. Front. Cell. Neurosci. **10**(July), 176 (2016). https://doi.org/10.3389/fncel.2016.00176
7. Galea, J.M., Albert, N.B., Ditye, T., Miall, C.: Disruption of the dorsolateral prefrontal cortex facilitates the consolidation of procedural skills. J. Cogn. Neurosci. **22**(6), 1158–1164 (2010). https://doi.org/10.1162/jocn.2009.21259
8. Geminiani, A., Casellato, C., Antonietti, A., D'Angelo, E., Pedrocchi, A.: A multiple-plasticity spiking neural network embedded in a closed-loop control system to model cerebellar pathologies. Int. J. Neural Syst. **28**, 1750017 (2017). https://doi.org/10.1142/S0129065717500174
9. Ghosh-Dastidar, S., Adeli, H.: A new supervised learning algorithm for multiple spiking neural networks with application in epilepsy and seizure detection. Neural Netw. **22**(10), 1419–1431 (2009). https://doi.org/10.1016/J.NEUNET.2009.04.003
10. Hadipour-Niktarash, A., Lee, C.K., Desmond, J.E., Shadmehr, R.: Impairment of retention but not acquisition of a visuomotor skill through time-dependent disruption of primary motor cortex. J. Neurosci. **27**(49), 13413–13419 (2007). https://doi.org/10.1523/JNEUROSCI.2570-07.2007
11. Luque, N.R., Garrido, J.A., Naveros, F., Carrillo, R.R., D'Angelo, E., Ros, E.: Distributed cerebellar motor learning: a spike-timing-dependent plasticity model. Front. Comput. Neurosci. **10**(March), 1–22 (2016). https://doi.org/10.3389/fncom.2016.00017
12. Miall, C., King, D.: State estimation in the cerebellum. Cerebellum **7**(4), 572–576 (2008). https://doi.org/10.1007/s12311-008-0072-6
13. Monaco, J., Casellato, C., Koch, G., D'Angelo, E.: Cerebellar theta burst stimulation dissociates memory components in eyeblink classical conditioning. Eur. J. Neurosci. **40**(July), 1–8 (2014). https://doi.org/10.1111/ejn.12700
14. Monaco, J., Rocchi, L., Ginatempo, F., D'Angelo, E., Rothwell, J.C.: Cerebellar theta-burst stimulation impairs memory consolidation in eyeblink classical conditioning. Neural Plast. **2018**, 1–8 (2018). https://doi.org/10.1155/2018/6856475
15. Ojeda, I.B., Tolu, S., Pacheco, M., Christensen, D.J., Lund, H.H.: A combination of machine learning and cerebellar-like neural networks for the motor control and motor learning of the fable modular robot. J. Robot. Netw. Artif. Life **4**, 62–66 (2017). https://doi.org/10.2991/jrnal.2017.4.1.14
16. Richardson, A.G., et al.: Disruption of primary motor cortex before learning impairs memory of movement dynamics. J. Neurosci. **26**(48), 12466–12470 (2006). https://doi.org/10.1523/JNEUROSCI.1139-06.2006
17. Ros, E., Carrillo, R.R., Ortigosa, E.M., Barbour, B., Agís, R.: Event-driven simulation scheme for spiking neural networks using lookup tables to characterize neuronal dynamics. Neural Comput. **18**(12), 2959–2993 (2006). https://doi.org/10.1162/neco.2006.18.12.2959
18. Tolu, S., Vanegas, M., Garrido, J.A., Luque, N.R., Ros, E.: Adaptive and predictive control of a simulated robot arm. Int. J. Neural Syst. **23**(3), 1350010 (2013). https://doi.org/10.1142/S012906571350010X